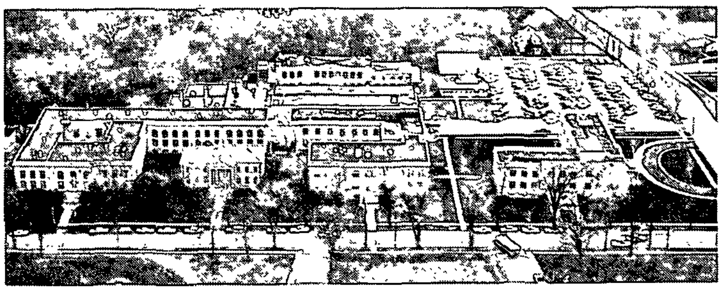

THE INSTITUTE OF PAPER CHEMISTRY, APPLETON, WISCONSIN

IPC TECHNICAL PAPER SERIES

NUMBER 274

FLASH X-RAY RADIOGRAPHY TECHNIQUES FOR VISUALIZING COATING FLOWS

NICK G. TRIANTAFILLOPOULOS AND THEODORE E. FARRINGTON, Jr.

JANUARY, 1988

Flash X-Ray Radiography Techniques for Visualizing Coating Flows

Nick G. Triantafillopoulos and Theodore E. Farrington, Jr.

Portions of this work were used by NGT as partial fulfillment of the requirements for the degree of Doctor of Philosophy from The Institute of Paper Chemistry. This paper is to be presented at the TAPPI Coating Conference in New Orleans on May 10-13, 1988

FLASH X-RAY RADIOGRAPHY TECHNIQUES FOR VISUALIZING COATING FLOWS

Nick G. Triantafillopoulos and
Theodore E. Farrington, Jr.
Graduate Student and Research Associate
The Institute of Paper Chemistry
Appleton, WI 54912

ABSTRACT

Flow visualization of opaque suspensions such as paper coating colors is not possible with photographic techniques. This paper presents a novel technique based on flash radiography which utilizes soft x-rays to visualize phenomena in coating flows. The main components of flash x-ray radiographic systems and the critical variables involved are described, with specific reference to imaging through coating colors. Results from two exploratory applications of this technique are illustrated. In the first, air entrainment in Couette flow is easily detected because the contrast between air and the color is high. In the second, streamlines of the laminar Couette flow are revealed by direct injection of tracing fluids, e.g., CMC solution saturated with sodium tungstate and lead acetate in glycerol. The total thickness of coating color penetrated is about 7 and 10 centimeters (approximately 4 inches), while spatial resolution is limited to approximately 100 microns. Finally, potential applications of the FXR technique are listed.

INTRODUCTION

Although theoretical analyses and computational fluid dynamics are two areas of fluid mechanics which have attracted considerable attention during the past few years, neither can replace physical experimentation. Flow visualization experiments still are among the best tools for studying fluid flow phenomena and testing the results of both theory and numerical simulation. In addition, such experiments have led to the discovery of numerous new flow phenomena. Conventional visualization techniques, however, are limited to materials transparent to light. Their application to opaque fluids, such as paper coating colors, is restricted by interposing material. This paper describes a novel experimental technique which utilizes x-rays to obtain images of coating flows.

Flow visualization of opaque suspensions containing particles at high concentrations is not possible with optical techniques based on light transmission, scattering, or reflectance. This is because light beams are disturbed by the suspended phase, due to refractive index variations and interparticular interferences. Hence most of the light between the measuring volume and a detector has been scattered (1). These effects will dominate when high-speed photography is applied in flows of dense dispersions containing particles with relatively high refractive index, such as the pigments used for paper coating. Similar constraints also exist in applications of pulsed lasers which are limited by spatial resolution and depth of field (1).

The limitations of optical techniques can be overcome by moving up the electromagnetic spectrum and using soft x-ray radiography. X-rays can easily penetrate fluids which are opaque to light and they are not substantially affected by concentration. For example, processes such as fuel injection (2) and kraft black liquor sprays (3) have been imaged with flash x-ray radiography. This technique utilizes high intensity x-ray pulses of 10 to 100 nanoseconds and energy levels of several hundred KeV to produce single stop-motion images of high speed phenomena. Comprehensive reviews of the technical details involved are described elsewhere (4,5).

Flash x-ray radiography (FXR) differs from conventional radiography in that the duration of the x-ray pulse, and therefore the exposure time, is extremely short and significantly less than any time constant of the dynamic phenomena to be studied. This added capability of time resolution carries, however, certain limitations (4). First, relatively high voltages are required to obtain adequate x-ray intensities during the very short period of a pulse. Second, very fast film and screen combinations must be used to achieve sharp images, since the intensity per pulse is limited. Third, large focal spot-size is required, since effective cooling of the x-ray generating target is impossible during a pulse, adversely affecting both spatial resolution and radiographic image sharpness. Finally, image enhancement cannot be adjusted during the exposure. Thus the effectiveness of FXR depends upon (a) selection of a system with x-ray energies appropriate for the desired application, (b) the x-ray absorption properties of the material to be radiographed, and (c) the optimization of radiographic variables, as these are interrelated in obtaining a high contrast, sharp image (6).

FXR systems comprise the pulsed beam generating unit and some kind of a detector (i.e., film) which transforms x-rays into visually observable images. The following sections outline basic features of FXR units, principal interactions of x-rays with matter, and present the results of exploratory visualization experiments of coating flows using FXR.

Flash X-Ray Systems Characteristics

X-ray generating units for flash radiography consist of two main parts: the x-ray tube and the pulsed high voltage source. Tubes for FXR produce relatively high peak current densities and effectively focus the electron beam by commonly utilized field emission technology (5). When high voltage is applied between the cathode (i.e., the emitter) and the anode (i.e., the x-ray target), electrons are "pulled" out of the metallic emitter by the very high electrical field created on its needle-like points (Fig. 1). Such a process leads to cathode surface vaporization and vacuum arc breakdown. Consequently, a maximum possible cathode emission occurs during the extremely short period of a pulse. The target is usually tungsten due to its high melting point, atomic number, and good electrical and thermal conductivities. A thin

1

Beryllium window can be employed in front of the tube which allows for low energy soft x-rays (e.g., below 5 KeV) to pass through, while Kovar windows can be used to filter them (7).

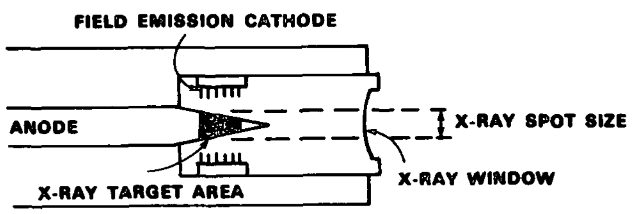

Fig. 1 Schematic of a common tube type for flash x-ray radiography.

Several techniques can be utilized to generate the pulsed high voltage and to accommodate the high current, low impedance characteristics of flash x-ray tubes (5). A common one is the Marx-Surge generator which consists of a bank of capacitors charged in parallel with a DC voltage and then discharged in series by means of cross-connected spark gaps. In more sophisticated systems, the capacitors are replaced by pulse-forming networks to produce a nearly rectangular output waveform which is more effective (4). The whole pulser is surrounded by a pressure vessel filled with nitrogen gas, while the gap spacing and gas pressure are adjusted to optimize the output discharge characteristics.

The primary x-ray beam emerging from the tube window contains a wide range of energies, or equivalently wavelengths, described by a continuous spectrum, the so-called bremsstrahlung. This spectrum contains hard (> 50 KeV), medium (20-50 KeV), soft (10-20 KeV), and ultrasoft (< 10 KeV) x-rays, with a peak at an energy level below 70 KeV and an asymptotic approach to zero at higher energies. Soft x-rays allow for higher dosage and better contrast, hence they are useful in observing low density objects (4). Hard x-rays, on the other hand, have greater penetrating power but lower contrast and, therefore, they are useful in radiographing high density media.

Two FXR systems, commercially available from Hewlett-Packard, McMinnville Division, are being evaluated at The Institute of Paper Chemistry. The first generates a 30 nanosecond pulse of 300 KeV x-rays and has an effective focal spot size of 5 mm with a dose of 55 milliroentgen (mR) at 38 cm. The second produces a 70 nanosecond pulse of 150 KeV x-rays with a 3 mm spot size and a dose of 40 mR at 20 cm. Both tubes have Beryllium windows to preserve the soft x-rays of the emerging beam, since these x-rays can be more effective in imaging relatively low density materials such as coating colors.

X-Rays Interaction with Matter and Radiographic Image

When x-rays strike or penetrate an object, some pass through and excite the film, others are absorbed, and some are scattered. Absorption of x-rays by matter is expressed by Beer's law (8):

$$I/Io = \exp(-\mu x) \qquad (1)$$

where Io is the incident x-ray intensity, I is the intensity remaining after passing through a thickness x of material, and μ is the linear mass attenuation (or absorption) coefficient characteristic of the material and its density. Beer's law assumes a narrow x-ray beam and monochromatic radiation. The primary x-ray beam emerging from a FXR tube, however, is by no means monochromatic but instead contains a wide range of wavelengths. As it travels through air and various thicknesses of other materials, soft x-rays absorb and scatter before having a chance to excite the film.

The linear x-ray absorption coefficient μ is made up of two components; one corresponds to photoelectric absorption and the other to Compton scattering (9). When the primary beam passes through matter, certain wavelengths are removed due to the photoelectric process, while the Compton effect scatters the beam, causing it to emerge at different angles. Photoelectric absorption, which is dominant for x-ray energies well below 100 KeV and depends on the atomic number of the penetrated material, leaves x-ray photons that create an image on the radiographic film (10). Compton scattering, which is dominant for x-ray energies above 100 KeV and depends on electron density, produces image fogging (11) and therefore is undesirable.

Flash x-ray radiographic images are recorded on film with or without intensifying screens, which serve the purpose of converting x-rays into optical photons. Many types of fast medical and industrial films, as well as screens, are available for radiography, and their selection depends on the specific application (11,12). Given a uniformly intense x-ray beam, density and/or thickness variations of the object under observation absorb different amounts of x-rays, thus creating areas with variable grayness on the film. The quality of a radiographic image is essentially determined by contrast, i.e., the depth resolution, and by definition, i.e., the lower limit of discernible details (5). In addition, spatial resolution is directly proportional to the focal size of the primary beam and to the relative position of the object with respect to the tube. Screens can be placed on the front or back of the film, but most commonly they are positioned on the backside to enhance image quality by sensitizing the film. Screens are more effective with increasing hardness, but they reduce spatial resolution.

Critical variables in FXR are the positioning of both the object and film with respect to the x-ray tube (Fig. 2). Object-to-film distance (OTFD) should be kept as short as possible to minimize image magnification and blur due to scattering. Source-to-object distance (STOD) is determined by the desired spatial resolution and contrast. Shorter STOD gives better penetration but it re-

2

duces spatial resolution. Other parameters which affect penetration are the type(s) of materials, which attenuate x-rays in their total path before reaching the film, and their respective thicknesses.

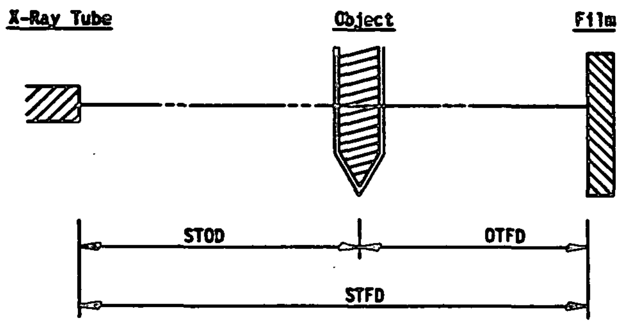

Fig. 2 Definition of the characteristic distances for flash x-ray radiography.

Application to Coating Flow Phenomena

As mentioned previously, x-rays of the primary beam propagate toward the detecting film while they interact with intervening matter through absorption and scattering. These interactions depend upon the x-rays' energy, the density of the object, and the atomic number of its constituent elements. Coating colors, the main absorbers of interest, contain elements of relatively low density and atomic number and are easily penetrated by x-rays. Because of these properties, however, radiographic contrast is reduced when using high energy radiation through large thicknesses of the absorber. Under these conditions, high scattering intensity increases the background exposure and hence deteriorates image quality. Such a limitation imposes constraints on both the x-ray source and the penetrating thickness.

At first, a study was conducted to determine the best x-ray source available for visualizing tracing wires embedded in a coating color. Figure 3 illustrates experimental results for x-ray doses through various absorber thicknesses for the high (300 KeV) and low (150 KeV) energy FXR systems. Although the high energy unit has better penetrating ability than the one with lower energy, contrast between the coating color and a 100-micron tungsten wire is very poor (Fig. 4). Tungsten has been used here as a demonstrative tracer for contrast because it has high density and atomic number; hence its linear mass x-ray absorption coefficient is much higher than that of the coating color.

Based on the above results, the 150 KeV Hewlett-Packard system is more appropriate for imaging coating flows. Spatial resolution, however, is limited by its focal spot size and the relative distances of both the object and film from the x-ray tube.

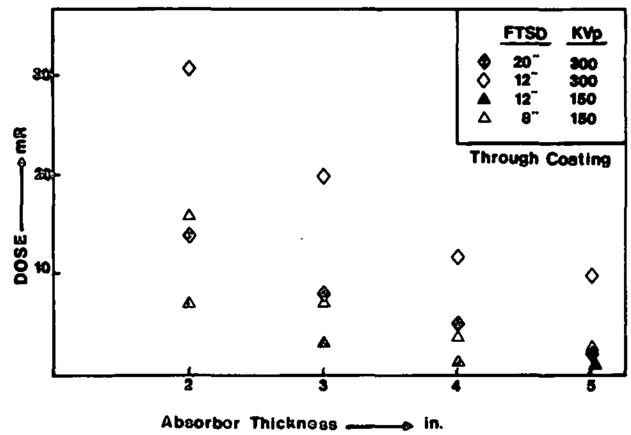

Fig. 3 Measured x-ray dosages at various film-to-source distances penetrating different thicknesses. The energy levels correspond to the two Hewlett-Packard units for flash x-ray radiography.

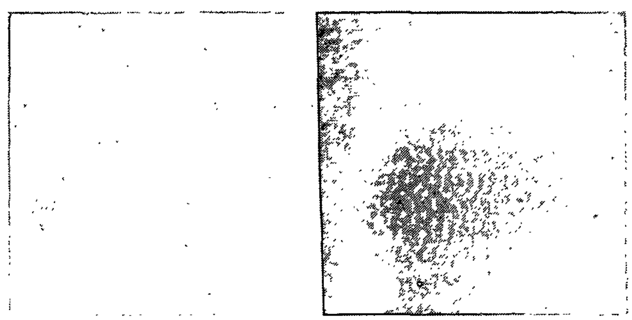

Fig. 4 Radiographs of a tungsten wire submerged vertically into a 4-inch wide fixture filled with a coating color. Using the high energy (left), and the low energy (right) systems.

After the selection of the x-ray system, radiographic parameters such as the film-to-source distance (FTSD) and the types of film and screens need to be determined. Experimental work (13) demonstrated that FTSD = 1.22 m (48 inches) with a Kodak XAR film backed by a Rarex Blue II screen gave the best image when visualizing the tungsten wire through 7-10 cm (approximately 3-4 inches) of absorber. Although the screen reduced both resolution and definition, it was required to enhance contrast, since the dose transmitted through 7 to 10 centimeters of color thickness was low, approximately 1 mR (Fig. 3). The spatial resolution, under these conditions, was limited to approximately 50 microns through 3 inches and 100 microns through 4 inches of coating color.

Radiographs of flow phenomena are obtained with coating colors (60% TS) flowing in a velocity-driven geometry. This is a Couette device made of Plexiglas, where the inner cylinder (9.33 cm diameter) rotates and the outer (10.34 cm diameter) remains restrained. Coating fluid is confined in

3

the annular gap (0.5 cm) between the two cylinders, and radiographs of the lower one-half of the rotating cylinder height (7.0 cm) are taken. The inner cylinder in this section is hollow and filled with coating fluid, so that x-rays are mainly absorbed by color. The film with the screen, both enclosed in a protective 12.7 x 17.8 centimeter (or 5 x 7 inch) casette, is placed in contact with the outer cylinder and on the opposite side from the x-ray source. Thus the maximum thickness of x-ray penetration is 10.8 centimeters (about 4-1/4 inches) in the center of the radiograph.

An initial application demonstrates how FXR can be used to observe air entrainment in coating flows, which is otherwise undetectable. The radiographs in Fig. 5 and 6 illustrate the experimental device empty and filled with water, respectively, to show differences in contrast. Figure 7 is a radiograph taken at 100 rpm while the annular gap was filled with coating contacting wall to wall. The radiograph in Fig. 8 represents the same setup, but it was obtained at a higher rotational speed, i.e., 900 rpm. This radiograph illustrates air entrainment next to the rotating inner cylinder, where air occupies not only regions of the cylindrical height but also areas on the bottom endface of the cylinder. The origin of this air is, most likely, the ambient atmosphere on the top free surface from where air can be sucked into the gap to displace fluid in contact with the rotating cylinder. Such a phenomenon has been previously reported in the literature (14) when shearing dense suspensions in coaxial cylinder geometries. It has been called the "cutting of hole" phenomenon and attributed to localized structural changes of the suspension which allow air to be sucked into the high velocity and low pressure region next to the rotating boundary (15).

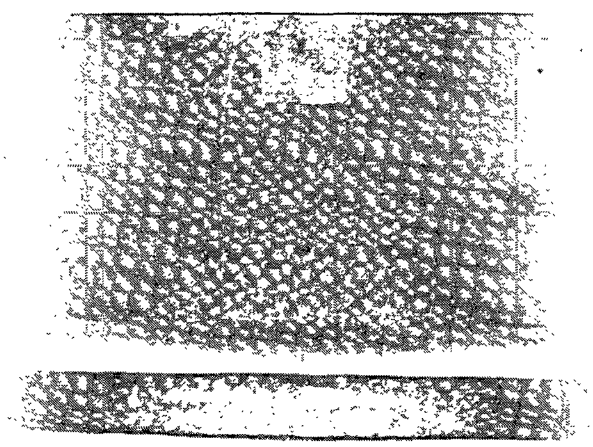

Fig. 5 A radiograph of a section of the Couette device when empty (0 rpm). Main absorber in the annular gap is air.

Another application of FXR is visualization of coating flows with qualitative global pictures. This can be achieved by injecting a tracing fluid into the flowing color and obtaining a single stop-motion image of the flow. An x-ray tracer is required because the chemical elements and substances comprising coating colors have relatively low atomic number and density, and therefore low linear mass x-ray absorption coefficients. If there is enough contrast between the tracer and coating color, e.g., the former having much higher linear x-ray absorption coefficient than the latter, characteristic lines can be revealed which have been defined to help describe the flow (i.e., streamlines, pathlines, or streaklines). Under steady state conditions, all these lines coincide and they form the characteristic streamlines of the flow. Retrieval of such information depends primarily on the density and viscosity of the tracing fluid and secondarily on the amount, location, and velocity of the injected stream (16).

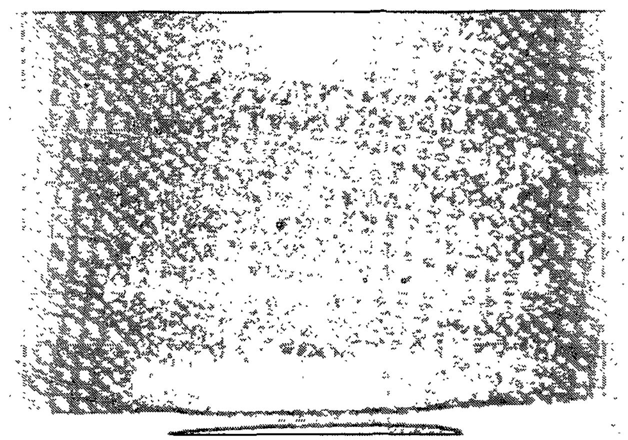

Fig. 6 A radiograph of a section of the Couette device filled with water (0 rpm).

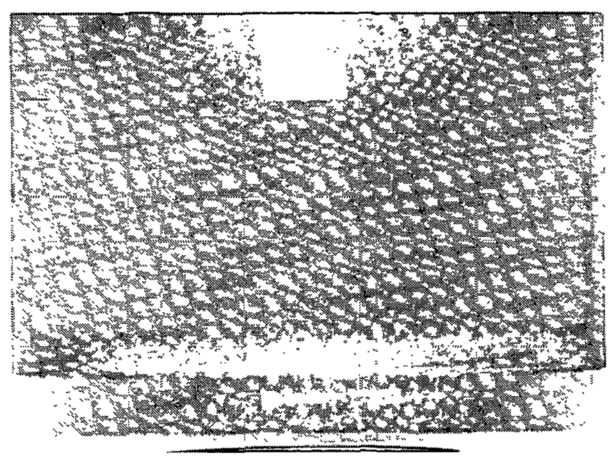

Fig. 7 A radiograph of a section of the Couette device filled with coating color. The inner cylinder rotates at 100 rpm.

Although the tracing fluid needs to contain elements with high x-ray attenuation (e.g., metal elements with high atomic number and density) for good contrast, it has to match the properties of the specific coating color. It is only then that the expectation for both fluids to behave similarly can be satisfied (16). Because of this require-

4

ment, however, there is a trade-off in the desired physical properties of tracing fluids. Characteristic linear x-ray absorption curves of tungsten, lead, and silver in the range of energies from 0 to 150 KeV are generated from values obtained from tables (17) and displayed in Fig. 9. All three elements have similar absorption at the useful range of 30-45 KeV with the 150 KeV unit (18), with the silver being slightly better.

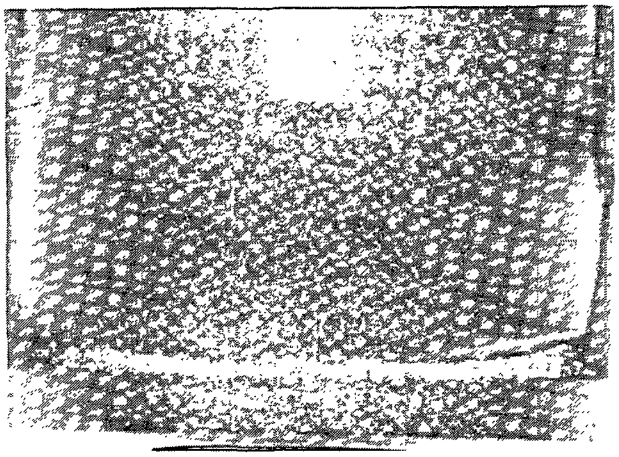

Fig. 8 A radiograph of a section of the Couette device filled with coating color. The inner cylinder rotates at 900 rpm.

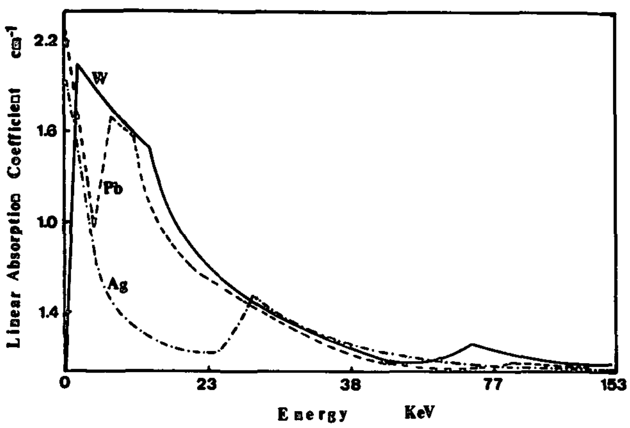

Fig. 9 Linear absorption coefficients for different x-ray energies in materials of various metallic elements.

Compounds of the above three elements were solubilized in water or glycerol and both their densities and viscosities were adjusted to be of the same order of magnitude as the ones of the coating color (1.56 g/cc, 890 cps @ 100 rpm Brookfield). Rheology was difficult to match precisely at all shear rates, since coating colors are shear thinning. Silver solutions, which had the best contrast, were not applicable because argentous ions (Ag+) reacted with the color and caused separation of the pigment from the suspension. A 4% CMC solution, saturated (62% b.w.) with sodium tungstate, and a lead acetate solution in glycerol successfully revealed the axisymmetric streamlines of laminar Couette flow (Fig. 10-12). The first had the same viscosity as the color, measured with a Brookfield viscometer at 100 rpm, while the second was 30% lower. These solutions were injected tangentially through a 1.56-mm-wide hole drilled on the outer cylindrical wall. Injection was achieved with an air pressure-driven cylinder which can deliver tracing solutions at velocities comparable to those of the coating color and up to about 1 m/sec.

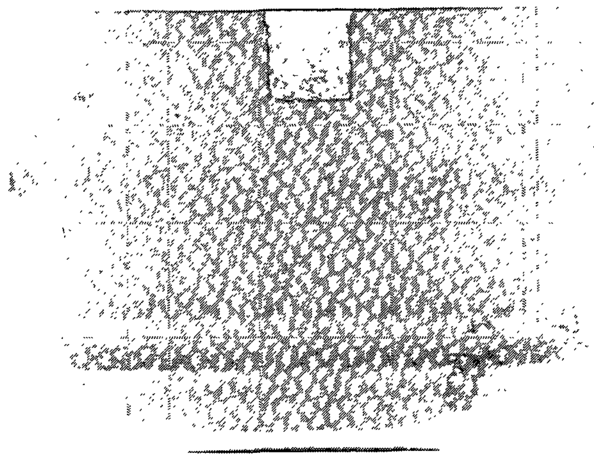

Fig. 10 A radiograph of a section of the Couette device filled with coating color. A stream of CMC solution, saturated with sodium tungstate, is injected along with direction of rotation (100 rpm, injection time = 5 seconds).

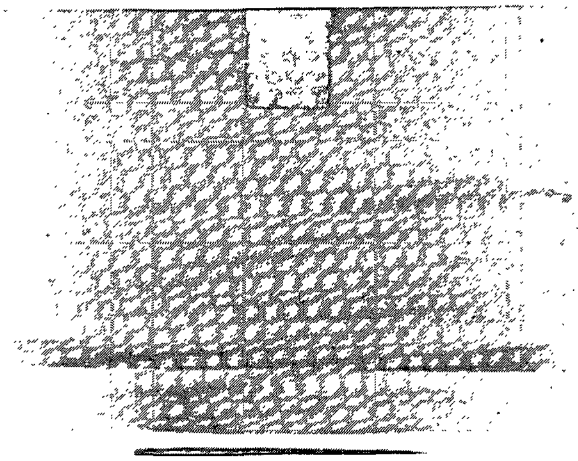

Fig. 11 A radiograph of a section of the Couette device filled with coating color. A stream of lead acetate in glycerol is injected along the direction of rotation (100 rpm, injection time = 5 seconds.)

5

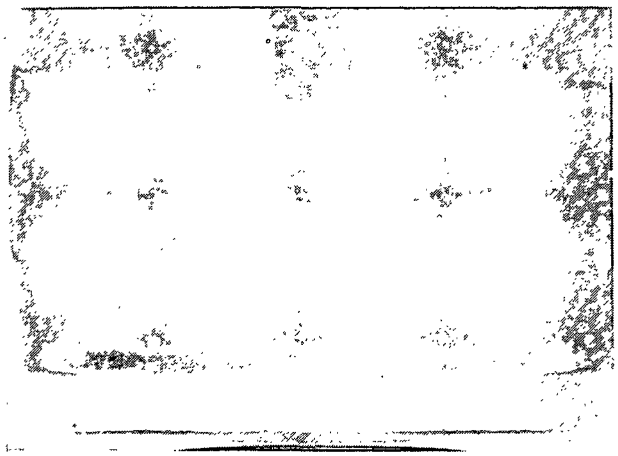

Fig. 12 A radiograph of a section of the Couette device filled with coating color. A stream of a CMC solution saturated with sodium tungstate is injected along the direction of rotation (900 rpm, injection time = 10 seconds).

CONCLUSIONS AND FUTURE WORK

It has been demonstrated that FXR can be a useful tool in studying flow phenomena of opaque coating fluids. Exploratory experiments have shown for the first time that air entrainment and streamlines can be visualized. Air entrainment observations in confined coating flows, through 7-10 centimeters (about 3-4 inches) depth of penetration, are easy because the radiographic contrast between air and coating colors is high. Visualization of streamlines, however, requires injection of appropriate tracing fluids.

FXR experiments can be utilized to test the application of proposed fluid mechanics theories and numerical results in well-defined flows of opaque fluids. This technique may also provide new insights for flow of coating colors in more complicated geometries such as the ones of industrial interest. It can also be a unique tool for observing dynamic contact angles when opaque fluids wet solid surfaces, such as the moving contact line upstream of a short-dwell puddle. At The Institute of Paper Chemistry, FXR will be utilized to study two- and three-dimensional flows of coating suspensions in rectangular lid-driven cavities, a model problem which can be simulated numerically.

ACKNOWLEDGMENTS

It is our pleasure to acknowledge the help and support above and beyond the call of duty of Dennis Spencer, who operated the x-ray unit and developed radiographs for this work.

This work was conducted by N.T. as partial fulfillment of the requirements for the Ph.D. degree at The Institute of Paper Chemistry, currently in progress.

REFERENCES

1. Norman, B., Moller, K., and Duffy, G. Hydrodynamics of papermaking fibres in water suspensions. Trans. Oxford Symp., Vol. 1, BPBIF, Sept., 1977. p. 195-245.

2. Bahl, K. L. and Vantine, H. C. A flash radiograph technique applied to fuel injection sprays. Proc. Flash Radiography Symp., (L. E. Bryant, ed.), ASNT, Columbus, OH, 1977. p. 193-200.

3. Farrington, T. E., Tappi J., to be published.

4. Carbonnier, F. Nondestructive Testing Handbook: Flash Radiography. ASNT, Columbus, OH, 1983.

5. Janet, F. and Thomer, G. Flash Radiography, Elsevier Publishing Co., Amsterdam, The Netherlands, 1976.

6. Flash X-Ray Seminar Notes, Hewlett-Packard, McMinnville Division, McMinnville, OR, 1987.

7. Flash Radiography, Technical Bulletin B-23, Hewlett-Packard, McMinnville Division, McMinnville, OR, 1973.

8. McCullough, E. C., Med. Phys. 3:307-315(1975).

9. Bertin, E. P. Principles and Practices of X-ray Spectrometric Analysis. Plenum Press, New York, 2nd edition, 1975. p. 51-68.

10. Vinegar, H. J. and Wellington, S. L., Rev. Sci. Instrum. 58(1):96-107(1987).

11. White, K. J. and McCoy, D. G. Influence of Scattering and Image Enhancement Technique for Flash X-rays Ballistic Events. Proc. Flash Radiography Symp. (L. E. Bryant, ed.), ASNT, Columbus, OH, 1984. p. 88-99.

12. Bryant, J. E. and Lucero, J. P. Film/Screen Study for Flash X-ray. Proc. Flash Radiography Symp., ASNT, Columbus, OH, 1984. p. 15-23.

13. Triantafillopoulos, N. G. A study of coating flows with flash x-ray radiography. Ph.D. thesis in progress. Progress Report Two, The Institute of Paper Chemistry, Appleton, WI, May, 1987.

14. Cheng, D. C.-H., Powder Technol. 37:255-273 (1984).

15. Patzold, R., Rheol. Acta 19:322-344(1980).

16. Mueller, T. J. Flow visualization by direct injection. In Fluid Mechanics Measurements (R. J. Goldstein, ed.), Hemisphere Publishing Co., Washington, DC, 1983. p. 307-375.

17. International Critical Tables, Vol. 1, McGraw-Hill Co., New York, NY, 1928. p. 8-15.

18. Farrington, T. E., Unpublished data, March, 1987.